




Clinicopathological and Molecular Characteristics of Macroscopically Yellowish-Colored Chromophobe Renal Cell Carcinoma Compared to Non-Yellowish-Colored Chromophobe Renal Cell Carcinoma

Clinical Pathology
Volume 14: 1–9
© The Author(s) 2021
Article reuse guidelines:
sagepub.com/journals-permissions
DOI: 10.1177/2632010X211064821


Fumiyoshi Kojima¹, Ibu Matsuzaki¹, Naoto Kuroda²,
Yurina Mikasa¹, Fidele Y Musangile¹, Ryuta Iwamoto¹,
Yuichi Takahashi¹, Akiko Matsubara³, Yasuo Kohjimoto⁴,
Isao Hara⁴ and Shin-ichi Murata¹

¹Department of Human Pathology, Wakayama Medical University, Wakayama, Japan.

²Department of Diagnostic Pathology, Kobe Kyodo Hospital, Nagata-ku, Kobe, Japan. ³Division of Human Pathology, Shiga University of Medical Science, Otsu, Shiga, Japan. ⁴Department of Urology, Wakayama Medical University, Wakayama, Japan.

ABSTRACT: Each histological variant of renal cell tumors has a unique color. The yellowish color of clear cell renal cell carcinoma (CCRCC) is explained by the presence of intracytoplasmic lipid and glycogen accumulation. Color changes in CCRCC are correlated with clinicopathological and metabolic changes, as well as biological behavior. We analyzed and compared the clinical, histopathological, and immunohistochemical features and gene expression profiles, in lipid metabolism of yellowish-colored ChRCC (ChRCC-Y), non-yellowish-colored ChRCC (ChRCC-N), and CCRCC. Of 14 ChRCCs, we retrieved 6 ChRCC-Ys. Patients with ChRCC-Y are younger than those with ChRCC-N, and the tumor is not predominant in males. ChRCC-Ys are smaller than ChRCC-Ns. Three ChRCC-Ys exhibited individual discrete tubule formation. No ChRCC-Ns exhibited individual discrete tubule formation. Two of 6 ChRCC-Ys showed relatively diffuse adipophilin positivity. No ChRCC-Ns demonstrated diffuse positivity for adipophilin. The expression of *SCD*, *FDFT1*, and *E2F1* showed a tendency to be lower in ChRCC-Y than in ChRCC-N. The expression of *PDGFB* showed a tendency to be higher in ChRCC-Y than in ChRCC-N. This study demonstrated ChRCC-Y did not indicate an increase in lipid and cholesterol metabolism and that ChRCC-Y did not have the common molecular alteration of CCRCC. The absence of such metabolic acceleration in ChRCC-Y might support the biological indolent behavior. Furthermore, we revealed that macroscopic color changes might be correlated with various clinicopathological features and immunohistochemical and molecular changes from different perspectives. We believe further characterization of RCC, including tumor heterogeneity, is needed to improve the management of patients with RCC.

KEYWORDS: Chromophobe renal cell carcinoma, lipid and cholesterol metabolism, color, adipophilin, mRNA expression

RECEIVED: May 12, 2021. **ACCEPTED:** November 17, 2021.

TYPE: Original Research

FUNDING: The author(s) received no financial support for the research, authorship, and/or publication of this article.

DECLARATION OF CONFLICTING INTERESTS: The author(s) declared no potential conflicts of interest with respect to the research, authorship, and/or publication of this article.

CORRESPONDING AUTHOR: Fumiyoshi Kojima, Department of Human Pathology, Wakayama Medical University, 811-1, Kimiidera, Wakayama, 641-8509, Japan. Email: fumiyosh@wakayama-med.ac.jp

Introduction

Each histological variant of renal cell tumors has a unique color and texture on the cut surface. For instance, clear cell renal cell carcinoma (CCRCC) is yellowish, papillary renal cell carcinoma (PRCC) is dirty and friable, chromophobe renal cell carcinoma (ChRCC) is beige in an unfixed state and gray/white in a fixed state, and renal oncocytoma is mahogany.^{1,2} However, in clinical practice CCRCC is often whitish or tan instead of yellowish. Similarly, ChRCC is sometimes yellowish on the cut surface, which confounds the diagnosis during macroscopic inspection³⁻⁵ Indeed, some variants of ChRCC including multicystic variant, neuroendocrine (NE) features, and NE-like features, have been reported to show a yellowish color.^{4,5} Variations in color can be interpreted as heterogeneity in renal cell carcinoma (RCC). Additionally, the color change in CCRCC suggests progression to high-grade RCC, which is often composed of eosinophilic cells with a high nuclear grade or shows a sarcomatoid change.

The yellowish color of CCRCC is explained by the intracytoplasmic fat and glycogen accumulation.^{1,2} CCRCC harbors a

VHL-HIF2a pathway alteration, which activates perilipin 2 (PLN2), CPT1A, SREBF1, and SREBF2 via KLF6 activation. Eventually, this results in lipid droplet accumulation.^{6,7} PLN2, also called adipophilin, is a lipid droplet coating protein. PLN2 is expressed throughout the body and in most CCRCCs.^{8,9} PLN2 expression is correlated with an adverse prognosis in some malignancies such as malignant melanoma, breast cancer, and pancreatic ductal adenocarcinoma.¹⁰⁻¹² However, in CCRCC, a decrease in PLN2 expression is correlated with a poor prognosis.^{8,13} In addition, high membranous fatty acid transport protein 4 expression is indicative of progressive disease.¹⁴ Thus, changes in lipid metabolism influence the biological behavior of various tumors.

Color changes in CCRCC are correlated with clinicopathological and metabolic changes, as well as biological behavior. However, there are no reports regarding the correlation between color and clinicopathological and molecular features in ChRCC. Here, we analyzed and compared the clinical, histopathological, and immunohistochemical features and gene



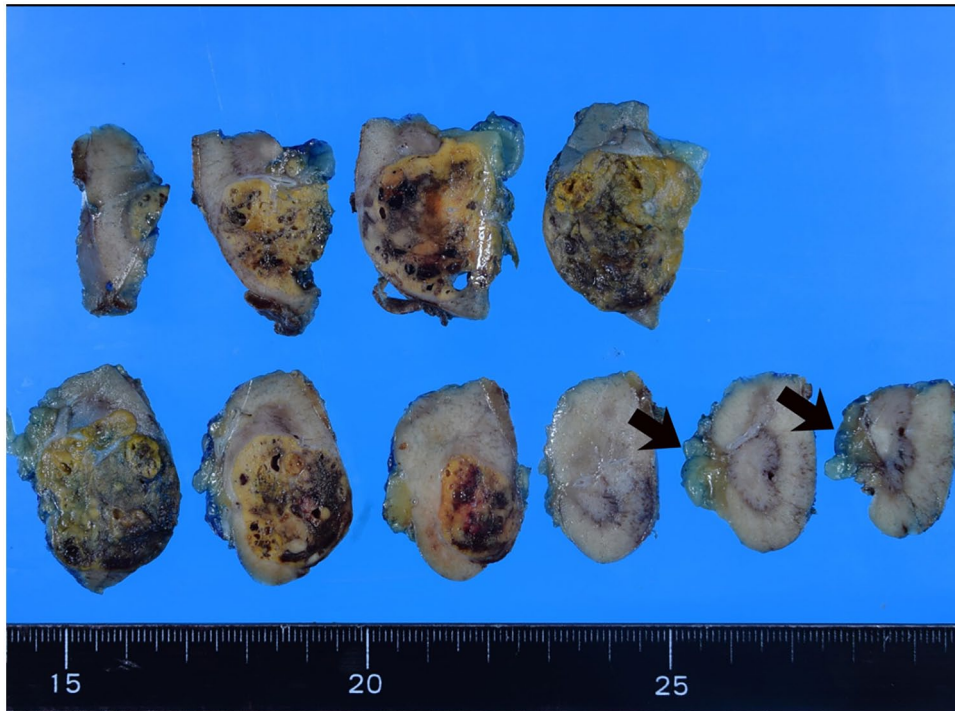


Figure 1. A representative macroscopic photo of yellowish-colored chromophobe renal cell carcinoma (ChRCC-Y). We defined ChRCC-Y had the color equivalent to or darker than perirenal fat color. The cut surface of this ChRCC was dark yellowish compared to the fat color (arrow) (case Y3).

expression profiles in lipid metabolism of yellowish-colored ChRCC (ChRCC-Y), non-yellowish-colored ChRCC (ChRCC-N), and CCRCC.

Materials and Methods

Case selection

The institutional ethics board approved this study. We reviewed macroscopic color photos of ChRCC available from our pathology report between 2015 and 2019 and collected ChRCCs in the HE findings and immunohistochemical results. We excluded ChRCCs that underwent preoperative transarterial embolization therapy because of the color change caused by hemorrhage or necrosis. We also excluded high-grade oncocytic tumors (renal cell carcinoma with eosinophilic and vacuolated cytoplasm), low-grade oncocytic tumors (c-kit-negative, CK7-positive), and unclassified oncocytic tumors.¹⁵⁻¹⁷ We classified ChRCC into ChRCC-Y or ChRCC-N. ChRCC-Y was defined as the color equivalent to or darker than perirenal fat color (Figure 1). The other ChRCCs without yellowish color were classified as ChRCC-N. We retrieved 6 ChRCC-Ys and 8 ChRCC-Ns. The largest ChRCC in the kidney was regarded as an index tumor. Non-neoplastic renal tissue from 4 ChRCC-Ys and 1 ChRCC-N were available for molecular analysis.

Clinical and pathological analysis

We obtained the patients' clinical information, including age, sex, tumor laterality, follow-up duration, and outcome, from electronic medical records. We evaluated the following

pathological findings: the color of the cut surface after fixation, tumor size, pT (AJCC eighth edition), tumor necrosis, lymphovascular invasion (LVI), tumor architecture, and cytological and stromal features (pigment and cholesterol deposition, hemorrhage, foamy macrophage, and edema). We evaluated the degree of glycogen accumulation, using Periodic acid/Schiff (PAS) staining and diastase digestion PAS (d-PAS) staining, based on the following proportion: 0, 0%; 1, less than 33%; 2, 33%–66%; 3, more than 66%. Immunohistochemistry was performed on 4 μ m-thick unstained slides using the Bond-III (Leica, Newcastle, UK) or BenchMark ULTRA (Roche, Basel, CH) auto-immunostainer according to the manufacturer's instructions. We used the following primary antibodies: vimentin (V9 mouse monoclonal, Roche, Basel, CH, ready-to-use [RTU], heat, pH9), c-kit (rabbit polyclonal, Dako, Tokyo, Japan, 1:200, heat, pH9), cytokeratin 7 (CK7) (SP52 rabbit monoclonal, Roche, Basel, CH, RTU, heat, pH9), SDHB (21A11AE7 mouse monoclonal, abcam, Tokyo, JPN, 1:400, heat, pH6), chromogranin A (LK2H10 mouse monoclonal, Roche, Basel, CH, RTU, heat, pH9), synaptophysin (MRQ-40 rabbit monoclonal, Roche, Basel, CH, RTU, heat, pH9), INSM-1 (A-8 mouse monoclonal, Santa Cruz Biotechnology, Dallas, TX, USA, 1:100, heat, pH9), and adipophilin (AP125 mouse monoclonal, Progen, Heidelberg, DE, 1:400, heat, pH9). Vimentin, c-kit, CK7, chromogranin A, and synaptophysin were processed using the BenchMark ULTRA. SDHB, INSM-1, and adipophilin were processed using Bond-III. The intensity of the stain was classified as weak, moderate, or strong. We evaluated the results using the H-score, which was calculated by multiplying the intensity score and the proportion (%).

Table 1. Clinical findings of chromophobe renal cell carcinoma.

CASE	AGE	SEX	SIDE	F/U (MONTH)	REC	PROGNOSIS	COMPLICATION
Y1	79	m	R	33	–	NED	
Y2	62	m	R	6	–	Lost	
Y3	65	m	R	6	–	NED	
Y4	67	f	R	3	–	NED	
Y5	53	f	L	9	–	NED	
Y6	87	f	R	25	–	NED	BHD s/o*
N1	81	m	R	10	–	NED	CCRCC, lung metastasis
N2	43	m	R	19	–	NED	
N3	64	m	R	34	–	NED	
N4	43	m	L	31	–	NED	
N5	66	f	R	16	–	DOA	PK
N6	68	m	R	18	–	Lost	
N7	58	m	L	1	–	NED	
N8	31	f	R	18	+	AWD	

Abbreviations: AWD, alive with disease; BHD s/o, suspicion of Bird-Hogg-Dube syndrome; CCRCC, clear cell renal cell carcinoma; DOA, died of another disease; f, female; f/u, duration of follow-up; L, left; m, male; NED, no evidence of disease; PK, pancreatic carcinoma; R, right; rec, recurrence;

*This patient had multiple small chromophobe renal cell carcinomas or chromophobe renal cell carcinoma-like lesions in the kidney.

We regarded H-score ≤ 50 as 0, $50 < \leq 100$ as 1, $100 < \leq 200$ as 2, and > 200 as 3.

Molecular analysis

Total RNA was extracted from formalin-fixed paraffin-embedded ChRCC or non-neoplastic renal tissue using the Maxwell® RSC Instrument (Promega Corporation, Madison, WI, USA) with the Maxwell RSC RNA FFPE Kit (Promega Corporation, Madison, WI, USA) according to the manufacturer's instructions. RNA quality was evaluated using a Quantus fluorometer (Promega Corporation, Madison, WI, USA) with QuantiFluor RNA Dye (E3310, Promega Corporation, Madison, WI, USA). Library construction and cDNA synthesis were performed using Illumina standard procedures. We used 100 ng of RNA and the AmpliSeq cDNA Synthesis for Illumina (Illumina, San Diego, CA, USA) to synthesize cDNA. RNA library preparation was performed using the AmpliSeq for Illumina custom RNA panel, AmpliSeq library PLUS for Illumina (Illumina, San Diego, CA, USA), and AmpliSeq CD indexes Set B for Illumina (Illumina, San Diego, CA, USA). The custom panel was composed of 19 genes, including one internal control gene (HPRT1). We investigated gene expression associated with fatty acid (*ACLY*, *ACACA*, *FASN*, *SCD*) and cholesterol synthesis (*HMGCR*, *FDPS*, *FDFT1*, *SQLE*, *CYP51A1*, *DHCR7*) and the gene expression of *LDLR* and *PLN2*. We also investigated the expression of genes associated

with lipid metabolism in CCRC (*KLF6*, *PDGFB*, *SREBF1*, *SREBF2*, *CPT1A*, and *E2F1*).^{6,7,18} RNA sequencing was performed using the iSeq100 (Illumina, San Diego, CA, USA) according to the manufacturer's instructions.

Statistical analysis

All statistical analyses were performed using JMP Pro 13 (SAS Institute, NC, USA). We statistically analyzed pathological and immunohistochemical data analyses between ChRCC-Y and ChRCC-N by the Fisher's exact test. Also, we statistically analyzed the mRNA expression data between ChRCC-Y and ChRCC-N, and between ChRCC-Y and non-neoplastic renal tissue using the Wilcoxon non-parametric test. *P*-value $\leq .05$ were considered statistically significant.

Results

Clinical findings (Table 1)

ChRCC-Y. Of 14 ChRCCs, we retrieved 6 ChRCC-Ys. The ages of the patients with ChRCC-Y ranged from 53 to 87 years (mean: 68.8 years, median: 66 years). Three males and 3 females had ChRCC-Y. Five ChRCC-Ys developed in the right kidney. All patients were alive without recurrence or metastasis. One patient with ChRCC-Y was suspected of having Bird-Hogg-Dube syndrome because of the presence of multiple small ChRCCs or ChRCC-like lesions in the kidney (case Y6).

Table 2. Pathological findings of chromophobe renal cell carcinoma.

CASE	COLOR	SIZE (CM)	PT	ARCHITECTURE	CYTOLOGICAL FINDINGS	LVI	NECROSIS	STROMA*	GLYCOGEN**
Y1	Yellow, dirty	3.5	1a	Tubulocystic	Eosin > reticular	-	-	Edematous, foam cells, cholesterolin	0
Y2	Deep yellow	2.5	1a	Solid, trabecular	Eosin	-	-	Edematous, hemorrhage	1
Y3	Deep yellow	3.6	3a	Tubulocystic	Eosin	-	-	Edema, cholesterolin, hemorrhage	1
Y4	Yellow	3.5	1a	Small tubule, solid	Eosin	-	-	Hemorrhage	3
Y5	Yellow	1.9	1a	Solid	Reticular	-	-	-	2
Y6	Yellow	2.5	1a	Tubulocystic	Eosin > reticular	-	-	Edematous, hemosiderin	3
N1	Beige	5.2	1b	Solid	Reticular > eosin	-	-	-	0
N2	Beige	2.9	1a	Solid	Eosin	-	-	-	2
N3	Beige	4.5	3a	Solid	Eosin	-	-	-	1
N4	Beige	2.5	1a	Solid	Eosin > reticular	-	-	-	1
N5	Mahogany brown	3	1a	Cribriform	Eosin	-	-	-	0
N6	Light brown	3.5	1a	Cribriform	Eosin	-	-	-	0
N7	Beige	5	1b	Solid	Eosin > reticular	-	+	Hemosiderin	1
N8	Beige	11.5	3a	Solid, sarcomatoid	Eosin	+	+	-	0

Abbreviations: eosin, eosinophilic; LVI, lymphovascular invasion.

*(-) almost no evaluable stroma and no significant findings.

**The degree of glycogen accumulation was evaluated using the following proportion: 0, none; 1, less than 33%; 2, 33%-66%; 3, 66%-100%.

ChRCC-N. Of 14 ChRCCs, we retrieved 8 ChRCC-Ns. The ages of the patients with ChRCC-N ranged from 31 to 81 years (mean: 56.8 years, median: 61 years). Six males and 2 females had ChRCC-N. Six ChRCC-Ns developed in the right kidney. Only 1 patient was administered with nivolumab plus ipilimumab because of the recurrence of ChRCC-N with a sarcomatoid change (case N8). One patient with ChRCC-N died of pancreatic carcinoma (case N5). The other patients were alive without recurrence or metastasis.

Morphological findings (Table 2)

ChRCC-Y. The tumor size of the ChRCC-Y ranged from 1.9 to 3.6 cm (mean: 2.9 cm, median: 3.0 cm). Five ChRCC-Ys were pT1a and 1 ChRCC-Y was pT3a. Four of the 6 ChRCC-Ys exhibited tubular formation, including tubulocystic growth pattern (Figure 2A) or small tubule formation (Figure 2B). Three of the ChRCC-Ys also showed individual discrete tubule formation. Two ChRCC-Ys exhibited solid growth (Figure 2C and D). Eosinophilic cells were predominant in ChRCC-Ys. One ChRCC-Y was eosinophilic variant (Figure 2C). One ChRCC

was composed of pale cells without apparent eosinophilic cell proliferation (Figure 2D). Three ChRCC-Ys showed moderate or strong glycogen accumulation (Figure 3). No ChRCC-Ys showed LVI or necrosis. Stromal edema was observed in 4 of 6 ChRCC-Ys (Figure 4A). Hemorrhage or cholesterolin deposition was found in 3 and 2 ChRCC-Ys, respectively (Figure 4A and B). Apparent foamy cells or hemosiderin deposition was present in 1 ChRCC-Y (Figure 4A and B).

ChRCC-N. The tumor size of the ChRCC-N ranged from 2.5 to 11.5 cm (mean: 4.8 cm, median: 4.0 cm). Eight ChRCC-Ns consisted of 4 pT1a, 2 pT1b, and 2 pT3a tumors. No ChRCC-N, including 2 ChRCC-Ns with cribriform growth patterns, showed individual discrete tubule formation. ChRCC-Ns included 4 classical variants (Figure 5A), 2 eosinophilic variants (Figure 5B), and 2 oncocytic variants (Figure 5C). Eosinophilic cells were predominant in ChRCC-Ns. One ChRCC-N showed moderate glycogen accumulation. One ChRCC-N showed LVI, and 2 ChRCC-Ns showed necrosis. None of the ChRCC-Ns, except for 1 ChRCC-N with hemosiderin deposition, had the previously mentioned stromal features.

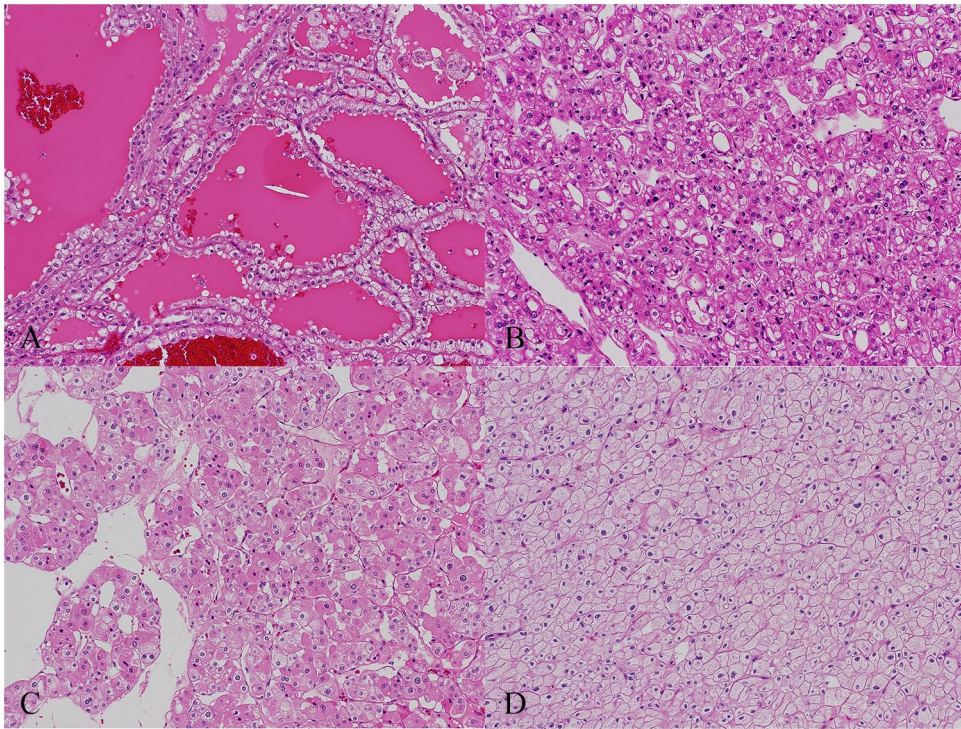


Figure 2. Representative histological features of yellowish-colored chromophobe renal cell carcinoma: (A) tubulocystic architecture composed of eosinophilic or oncocytic cells (case Y1, 3, and 6), (B) acinar growth pattern with small tubules or intracytoplasmic vacuoles (case Y4), (C) solid growth composed of eosinophilic cells (case Y2), and (D) solid growth composed of large pale cells (case Y5).

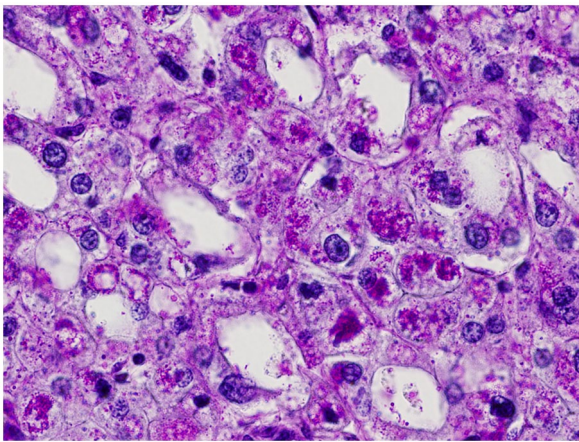


Figure 3. A representative PAS staining in chromophobe renal cell carcinoma. There were many intracytoplasmic PAS positive granules (glycogen) which were digested by diastase (case Y4).

Immunohistochemical findings (Table 3)

ChRCC-Y. All ChRCC-Ys were negative for vimentin and positive for c-kit (Figure 6A and B). Two of 6 ChRCC-Ys exhibited diffuse and strong positivity for CK7 (Figure 6C). All ChRCCs, except for 1 ChRCC-Y, were completely negative for NE markers. A few tumor cells in the ChRCC-Y (case Y1) were weakly stained for synaptophysin. However, additional immunohistochemical staining for INSM-1 was negative. SDHB was preserved in all ChRCCs. All ChRCC-Ys had positive cells for adipophilin (Figure 6D). However, the adipophilin-positive cells in the tumor occupied a very small area.

Only 2 ChRCC-Ys showed more than 10% adipophilin-positive cells.

ChRCC-N. Six of 8 ChRCC-Ns were completely negative for vimentin, 4 of 8 ChRCC-Ns showed moderate positivity for c-kit, and 7 of 8 ChRCC-Ns showed moderate or strong positivity for CK7. All ChRCC-Ns were completely negative for NE markers. Four of 8 ChRCC-Ns had positive cells for adipophilin. However, the positive cells occupied less than 5% of the tumors.

Statistical analyses (Supplemental table)

ChRCC-Y typically showed discrete tubule formation and stromal features ($P = .0150$ and $.0256$, respectively). There were no significant differences about the other pathological and immunohistochemical findings. The expression of *SCD*, *FDFT1*, and *E2F1* was significantly lower in ChRCC-Y than in ChRCC-N ($P = .0169$, $.0332$, $.0454$, respectively) (Figure 7A). Also, the expression of *PDGFB* was significantly higher in ChRCC-Y than in ChRCC-N ($P = .0239$) (Figure 7A). The mRNA expressions of *FDPS*, *FDFT1*, *SQLE*, *PLN2*, and *KLF6* in ChRCC-Y were significantly lower than in non-neoplastic renal tissue ($P = .0358$, $.0081$, $.0225$, $.0225$, $.0225$, respectively) (Figure 7B).

Discussion

Patients with RCC develop resistance to various therapies because RCC has intratumoral heterogeneity.^{19,20} The

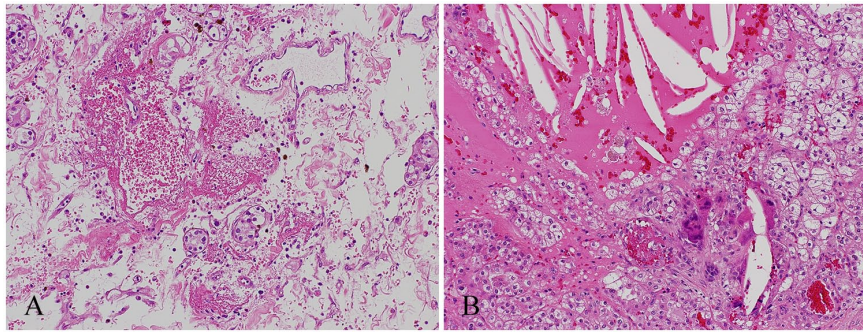


Figure 4. Representative stromal findings of chromophobe renal cell carcinoma (ChRCC): (A) hem siderin deposition and hem siderin-laden macrophages were present in the edematous stroma with hemorrhage (case Y6) and (B) there was cholesterol deposition (case Y1).

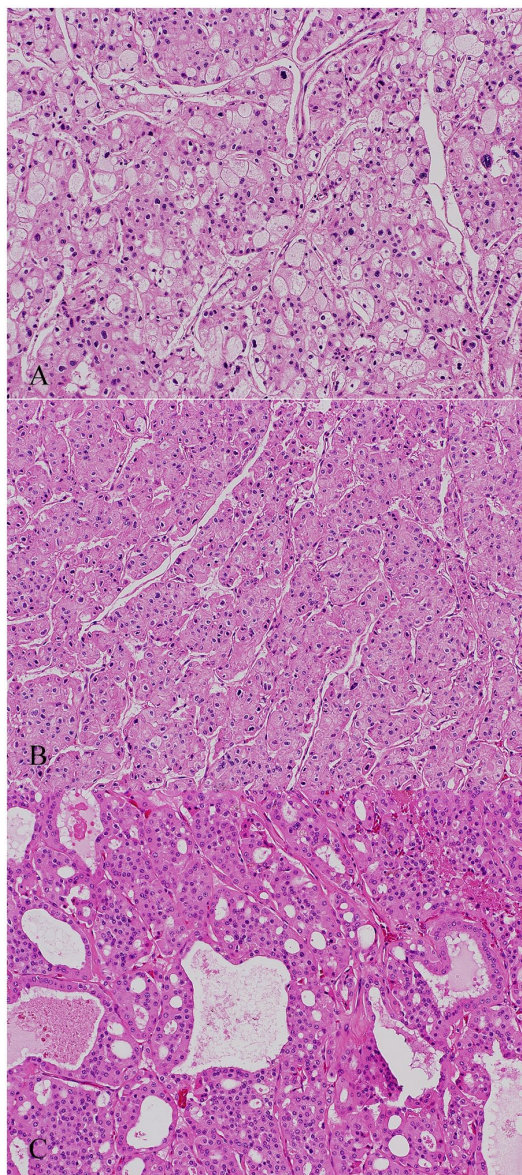


Figure 5. Representative histological features of non-yellowish-colored chromophobe renal cell carcinoma (ChRCC-N): (A) classical pattern (case N1, 4, and 7). Plant-like cells and eosinophilic cells showed sheet-like growth, (B) eosinophilic variant (case N2, 3, and 8). Eosinophilic cells showed sheet-like and thick trabecular growth. The cells had perinuclear halo and nucleus with irregular contour, and (C) oncocytic variant (case N5 and 6). This tumor showed cribriform growth pattern composed of oncocytic cells.

heterogeneity in CCRCC is observed as a macroscopic color and from tumor architecture and cytological and immunohistochemical findings.^{21,22} ChRCC exhibits similar heterogeneity, and various histological variants have been reported such as eosinophilic, pigmented adenomatoid, microcystic, oncocytic, multicystic, NE, and NE-like features.^{3-5,23,24} However, those variants have not been correlated with the biological behavior of ChRCC. Tumor size, stage, necrosis, LVI, and sarcomatoid change are predictors of ChRCC.^{25,26} Lipid/cholesterol metabolic perturbation among ChRCC should be clarified to obtain additional therapeutic strategies and predictive markers.

Patients with ChRCC-Y are younger than those with ChRCC-N, and the tumor is not predominant in males. The findings that ChRCC-Ys are smaller in size and have neither necrosis nor LVI suggest that ChRCC-Ys are more indolent behavior than ChRCC-N. Most ChRCC-Ys showed tubule formation. Tubule formation is atypical for ChRCC. Such ChRCC-Ys may be classified as multicystic or microcystic ChRCC, some of which have been reported as yellowish.^{3,4} Three of 6 ChRCC-Ys were composed of individual discrete, well-formed tubulocystic architecture, contrary to previously reported microcystic ChRCC that included various adenomatous architectures such as cribriform, fused adenomatous, and small acini. However, most ChRCC-Ns were the classical or eosinophilic type.

Immunohistochemically, the results of c-kit and CK7 were different between ChRCC-Y and ChRCC-N. Some ChRCC with NE or NE-like features have been reported to show a yellowish color. However, neither ChRCC-Ys nor ChRCC-Ns exhibited NE features in this study. Some ChRCC-Ys showed relatively diffuse adipophilin positivity. No ChRCC-Ns had diffuse positivity for adipophilin. The presence of adipophilin in ChRCC-Ys suggests intracytoplasmic lipid droplet accumulation. However, adipophilin expression at the protein level did not correlate with that at the mRNA level in this study. One possible reason for this is the high sensitivity of immunohistochemistry. Another possible reason is that some ChRCC-Ys cannot degrade adipophilin efficiently; thus, the half-life is longer, and adipophilin accumulates in the tumor cells in the absence of an increase in PLN2 mRNA expression.

Yao et al⁸ demonstrated lower expression of adipose differentiation-related proteins at the mRNA and protein levels in

Table 3. Immunohistochemical findings of chromophobe renal cell carcinoma.

CASE	VIMENTIN	C-KIT	CK7	SDHB	CHROMOGRANIN A	SYNAPTOPHYSIN	ADIPOPHILIN (%)
Y1	0	2	0	Intact	0	0*	30
Y2	0	1	3	Intact	0	0	5
Y3	0	1	1	Intact	0	0	<5
Y4	0	2	3	Intact	0	0	<5
Y5	0	3	1	Intact	0	0	<5
Y6	0	2	0	Intact	0	0	60
N1	0	2	2	Intact	0	0	0
N2	0	2	2	Intact	0	0	<5
N3	0	2	3	Intact	0	0	<5
N4	0	0	0	Intact	0	0	<5
N5	1	0	2	Intact	0	0	0
N6	1	0	3	Intact	0	0	0
N7	0	2	3	Intact	0	0	5
N8	0	0	2	Intact	0	0	0

*Y1 showed weak positivity for synaptophysin (H-score: 0), but both chromogranin A and INSM1 were negative.

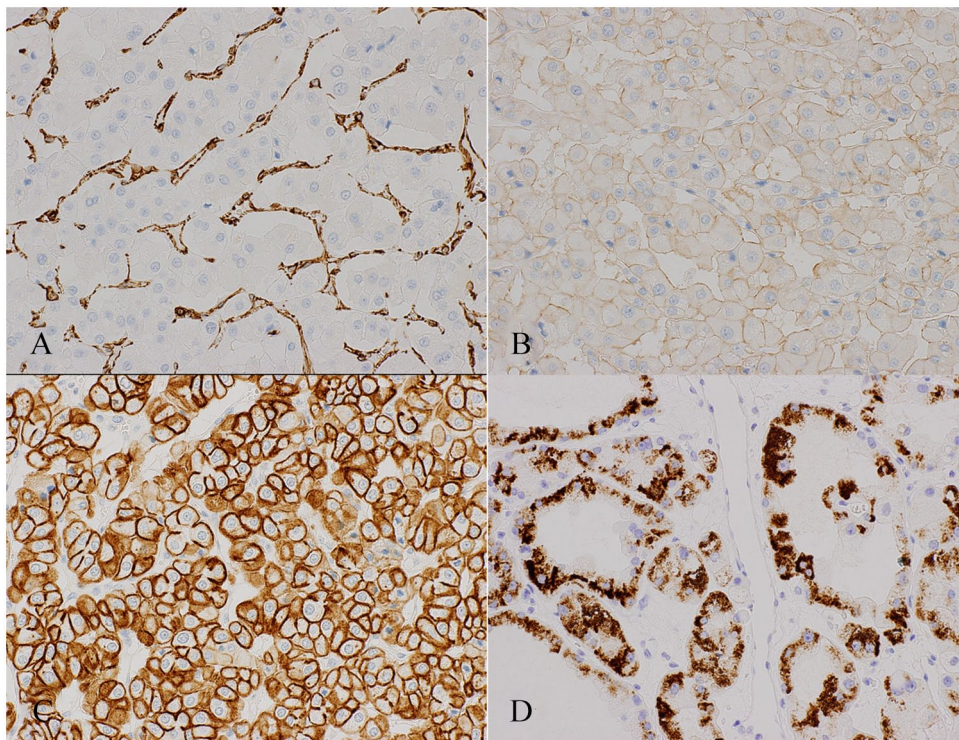


Figure 6. Representative immunohistochemical findings of chromophobe renal cell carcinoma (ChRCC): (A) all ChRCCs were negative for vimentin (case Y2), (B) most ChRCCs showed membranous positivity for c-kit (case Y2), (C) ChRCC typically showed diffuse strong positivity for CK7 (case Y2), and (D) some ChRCCs showed positivity for adipophilin (case Y6).

ChRCC compared to the expression in CCRCC. However, this study did not consider the heterogeneity of ChRCC cases. In our study, we classified the ChRCC cases into 2

groups, yellowish and non-yellowish, based on the color of the cut surface. In CCRCC, an increase in *KLF6* expression by *VHL-HIF2* axis alteration accelerates *PDGFB* expression and

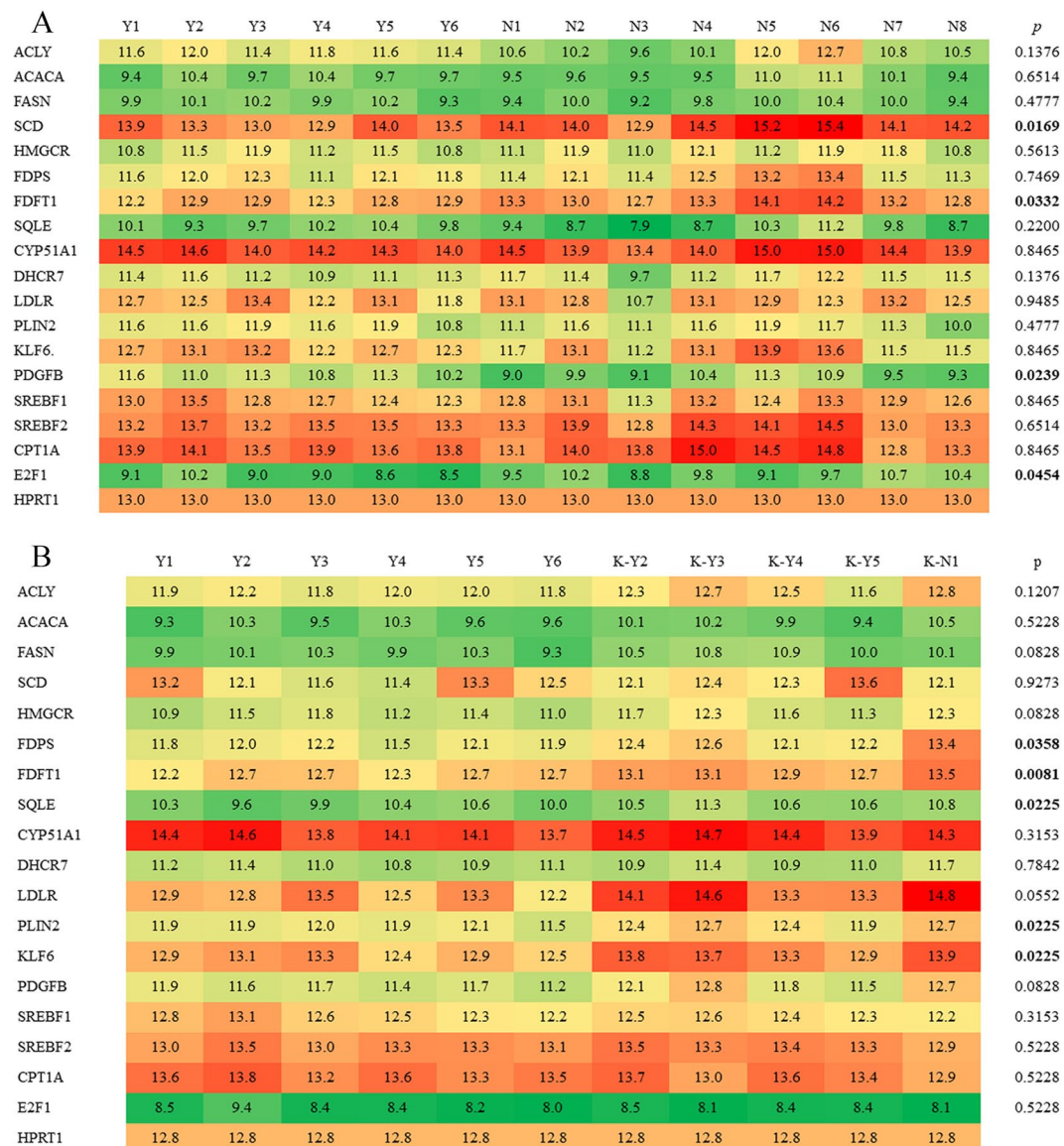


Figure 7. Heat map of mRNA expression of (A) yellowish-colored chromophobe renal cell carcinoma (ChRCC-Y) and non-yellowish-colored chromophobe renal cell carcinoma (ChRCC-N), and (B) ChRCC-Y and non-neoplastic renal tissue. Some gene expressions between (A) ChRCC-Y and ChRCC-N (SCD, FDFT1, E2F1), and between (B) ChRCC-Y and non-neoplastic tissue (FDPS, FDFT1, SQLE, PLIN2, KLF6) showed a different tendency, respectively.

decreases *E2F1* expression. *KLF6* suppresses lipid metabolism regulators, thereby increasing lipid metabolism and decreasing *E2F1* expression.¹⁸ In this study, the expression of upstream and downstream metabolites of *PDGFB* and *E2F1*, including *KLF6*, *SREBF1*, and *SREBF2*, did not increase in ChRCC-Ys. This suggested a different mechanism for lipid metabolism between ChRCC-Y and CCRCC.

Additionally, both *SCD* mRNA expression, which is involved in the final process of phospholipid and triacylglyceride metabolism, and *FDFT1* mRNA expression, which is involved in cholesterol synthesis, were lower in ChRCC-Ys than in ChRCC-Ns. Furthermore, there was a low expression of some genes associated with cholesterol metabolism in ChRCC-Y compared to non-neoplastic renal parenchyma. These results support the absence of lipid and cholesterol metabolism acceleration in

ChRCC-Y. Inactive metabolic states in ChRCC-Ys likely reflect indolent biological features, and lipid/cholesterol targeted therapies are not effective for ChRCC-Y.

The reason why ChRCC is yellowish is difficult to specify. One possibility is intracytoplasmic lipid accumulation. The presence of adipophilin in some of the ChRCC-Ys suggests intracytoplasmic lipid droplet accumulation and may contribute to the yellowish color of ChRCC. Foamy macrophages in the cysts and edematous stroma might also influence the color of some ChRCCs. Another possibility for yellowish ChRCC is intracytoplasmic glycogen accumulation. However, ChRCC shows low glycogen accumulation.^{27,28} Similar to previous reports, most ChRCCs in this study showed mild or no glycogen accumulation, but strong glycogen accumulation was demonstrated in some ChRCC-Ys.

This study has some limitations. First, the sample size was small because it was difficult to retrieve evaluable and strikingly colored photos. Second, we could not analyze all the enzymes relevant to lipid/cholesterol metabolism and confirm the protein level expression of metabolites.

Conclusion

This study suggested that ChRCC-Y did not indicate an increase in lipid and cholesterol metabolism and that ChRCC-Y did not have the common molecular alteration of CCRCC. The absence of such metabolic acceleration in ChRCC-Y might support the indolent biological behavior. Furthermore, we revealed that macroscopic color changes might be correlated with various clinicopathological features and immunohistochemical and molecular changes from different perspectives. We believe further characterization of RCC, including tumor heterogeneity, is needed to improve the management of patients with RCC.

Acknowledgements

We thank Kobayashi M., C. T. and Yokozeki N., C. T. for their pathological technical support.

Author Contributions

Fumiyoshi Kojima: Conceptualization, Methodology, Formal Analysis, Data Curation, Writing – Original Draft, and Project Administration. Ibu Matsuzaki and Fidel Y. Musangile: Methodology, Investigation, and Formal Analysis. Yurina Mikasa and Ryuta Iwamoto: Investigation. Yasuo Kohjimoto: Resources. Yuichi Takahashi, Yoshifumi Iwahashi, and Kenji Warigaya: Supervision. Akiko Matsubara and Naoto Kuroda: Resources and Supervision. Isao Hara and Shin-ichi Murata: Writing-Review and Editing.

Ethics

Informed consent was obtained in the form of opt-out on the web-site. Those who rejected were excluded. We have been approved by our institutional ethics committee (Research ethics committee of Wakayama Medical University).

ORCID iDs

Fumiyoshi Kojima  <https://orcid.org/0000-0002-9478-9692>

Ibu Matsuzaki  <https://orcid.org/0000-0002-5096-5850>

Supplemental material

Supplemental material for this article is available online.

REFERENCES

- Amin MB, Grignon DJ, Srigley JR, Eble JN. *Urological Pathology*. Lippincott Williams and Wilkins, a Wolters Kluwer; 2014.
- Bostwick DG, Cheng L. *Urologic Surgical Pathology*. Elsevier Saunders; 2014.
- Foix MP, Dunatov A, Martinek P, et al. Morphological, immunohistochemical, and chromosomal analysis of multicystic chromophobe renal cell carcinoma, an architecturally unusual challenging variant. *Virchows Arch*. 2016;469:669-678.
- Gutiérrez FJQ, Panizo Á, Tienza A, et al. Cytogenetic and immunohistochemical study of 42 pigmented microcystic chromophobe renal cell carcinoma (PMChRCC). *Virchows Arch*. 2018;473:209-217.
- Peckova K, Martinek P, Ohe C, et al. Chromophobe renal cell carcinoma with neuroendocrine and neuroendocrine-like features. Morphologic, immunohistochemical, ultrastructural, and array comparative genomic hybridization analysis of 18 cases and review of the literature. *Ann Diagn Pathol*. 2015;19:261-268.
- Syafuruddin SE, Rodrigues P, Vojtasova E, et al. A KLF6-driven transcriptional network links lipid homeostasis and tumour growth in renal carcinoma. *Nat Commun*. 2019;10:1152.
- Du W, Zhang L, Brett-Morris A, et al. HIF drives lipid deposition and cancer in ccRCC via repression of fatty acid metabolism. *Nat Commun*. 2017;8:1769.
- Yao M, Tabuchi H, Nagashima Y, et al. Gene expression analysis of renal carcinoma: adipose differentiation-related protein as a potential diagnostic and prognostic biomarker for clear-cell renal carcinoma. *J Pathol*. 2005;205:377-387.
- Sztralzyd C, Kimmel AR. Perilipins: lipid droplet coat proteins adapted for tissue-specific energy storage and utilization, and lipid cytoprotection. *Biochimie*. 2014;96:96-101.
- Fujimoto M, Matsuzaki I, Nishitsuji K, et al. Adipophilin expression in cutaneous malignant melanoma is associated with high proliferation and poor clinical prognosis. *Lab Invest*. 2020;100:727-737.
- Kuniyoshi S, Miki Y, Sasaki A, et al. The significance of lipid accumulation in breast carcinoma cells through perilipin 2 and its clinicopathological significance. *Pathol Int*. 2019;69:463-471.
- Hashimoto Y, Ishida M, Ryota H, et al. Adipophilin expression is an indicator of poor prognosis in patients with pancreatic ductal adenocarcinoma: an immunohistochemical analysis. *Pancreatology*. 2019;19:443-448.
- Tolkach Y, Lüders C, Meller S, Jung K, Stephan C, Kristiansen G. Adipophilin as prognostic biomarker in clear cell renal cell carcinoma. *Oncotarget*. 2017;8:28672-28682.
- Kim YS, Jung J, Jeong H, et al. High membranous expression of fatty acid transport protein 4 is associated with tumorigenesis and tumor progression in clear cell renal cell carcinoma. *Dis Markers*. 2019;2019:5702026.
- He H, Trpkov K, Martinek P, et al. "High-grade oncocytic renal tumor": morphologic, immunohistochemical, and molecular genetic study of 14 cases. *Virchows Arch*. 2018;473:725-738.
- Chen YB, Mirsadraei L, Jayakumaran G, et al. Somatic mutations of TSC2 or MTOR characterize a morphologically distinct subset of sporadic renal cell carcinoma with eosinophilic and vacuolated cytoplasm. *Am J Surg Pathol*. 2019;43:121-131.
- Trpkov K, Williamson SR, Gao Y, et al. Low-grade oncocytic tumour of kidney (CD117-negative, cytokeratin 7-positive): a distinct entity? *Histopathology*. 2019;75:174-184.
- Gao Y, Li H, Ma X, et al. KLF6 suppresses metastasis of clear cell renal cell carcinoma via transcriptional repression of E2F1. *Cancer Res*. 2017;77:330-342.
- López JI. Intratumor heterogeneity in clear cell renal cell carcinoma: a review for the practicing pathologist. *APMIS*. 2016;124:153-159.
- López JI, Cortés JM. Multisite tumor sampling: a new tumor selection method to enhance intratumor heterogeneity detection. *Hum Pathol*. 2017;64:1-6.
- Kojima F, Bulimbasic S, Alaghebandan R, et al. Clear cell renal cell carcinoma with paneth-like cells: clinicopathologic, morphologic, immunohistochemical, ultrastructural, and molecular analysis of 13 cases. *Ann Diagn Pathol*. 2019;41:96-101. Aug 2019;41:96-101.
- Zaldumbide L, Erramuzpe A, Guarch R, Cortés JM, López JI. Large (>3.8 cm) clear cell renal cell carcinomas are morphologically and immunohistochemically heterogeneous. Comparative Study Multicenter Study. *Virchows Arch*. 2015;466:61-66.
- Kuroda N, Tanaka A, Yamaguchi T, et al. Chromophobe renal cell carcinoma, oncocytic variant: a proposal of a new variant giving a critical diagnostic pitfall in diagnosing renal oncocytic tumors. *Med Mol Morphol*. 2013;46:49-55.
- Hes O, Vanecek T, Perez-Montiel DM, et al. Chromophobe renal cell carcinoma with microcystic and adenomatous arrangement and pigmentation—a diagnostic pitfall. Morphological, immunohistochemical, ultrastructural and molecular genetic report of 20 cases. *Virchows Arch*. 2005;446:383-393.
- Amin MB, Paner GP, Alvarado-Cabrero I, et al. Chromophobe renal cell carcinoma: histomorphologic characteristics and evaluation of conventional pathologic prognostic parameters in 145 cases. *Am J Surg Pathol*. 2008;32:1822-1834.
- Przybycin CG, Cronin AM, Darvishian F, et al. Chromophobe renal cell carcinoma: a clinicopathologic study of 203 tumors in 200 patients with primary resection at a single institution. *Am J Surg Pathol*. 2011;35:962-970.
- Thoenes W, Störkel S, Rumpelt HJ, Moll R, Baum HP, Werner S. Chromophobe cell renal carcinoma and its variants—a report on 32 cases. *J Pathol*. 1988;155:277-287.
- Krishnan B, Truong LD. Renal epithelial neoplasms: the diagnostic implications of electron microscopic study in 55 cases. *Hum Pathol*. 2002;33:68-79.